NANO LETTERS

Letter

pubs.acs.org/NanoLett

Enhanced Amplified Spontaneous Emission in Perovskites Using a Flexible Cholesteric Liquid Crystal Reflector

Samuel D. Stranks,*[,†] Simon M. Wood,[‡] Konrad Wojciechowski,[†] Felix Deschler,[§] Michael Saliba,[†] Hitesh Khandelwal,[⊥] Jay B. Patel,[†] Steve J. Elston,[‡] Laura M. Herz,[†] Michael B. Johnston,[†] Albertus P. H. J. Schenning,[⊥] Michael G. Debije,[⊥] Moritz K. Riede,[†] Stephen M. Morris,*[,‡] and Henry J. Snaith*[,†]

[†]Clarendon Laboratory, University of Oxford, Parks Road, Oxford OX1 3PU, U.K.

[‡]Department of Engineering Science, University of Oxford, Parks Road, Oxford OX1 3PJ, U.K.

[§]Cavendish Laboratory, University of Cambridge, J J Thomson Avenue, Cambridge CB3 0HE, U.K.

[⊥]Department of Chemical Engineering and Chemistry, Eindhoven University of Technology, P.O. Box 513, Eindhoven, 5600 MB, The Netherlands

Supporting Information

ABSTRACT: Organic−inorganic perovskites are highly promising solar cell materials with laboratory-based power conversion efficiencies already matching those of established thin film technologies. Their exceptional photovoltaic performance is in part attributed to the presence of efficient radiative recombination pathways, thereby opening up the possibility of efficient light-emitting devices. Here, we demonstrate optically pumped amplified spontaneous emission (ASE) at 780 nm from a 50 nm-thick film of $CH_3NH_3PbI_3$ perovskite that is sandwiched within a cavity composed of a thin-film (~7 μm) cholesteric liquid crystal (CLC) reflector and a metal back-reflector. The threshold fluence for ASE in the perovskite film is reduced by at least two orders of magnitude in the presence of the CLC reflector, which results in a factor of two reduction in threshold fluence compared to previous reports. We consider this to be due to improved coupling of the oblique and out-of-plane modes that are reflected into the bulk in addition to any contributions from cavity modes. Furthermore, we also demonstrate enhanced ASE on flexible reflectors and discuss how improvements in the quality factor and reflectivity of the CLC layers could lead to single-mode lasing using CLC reflectors. Our work opens up the possibility of fabricating widely wavelength-tunable "mirror-less" single-mode lasers on flexible substrates, which could find use in applications such as flexible displays and friend or foe identification.

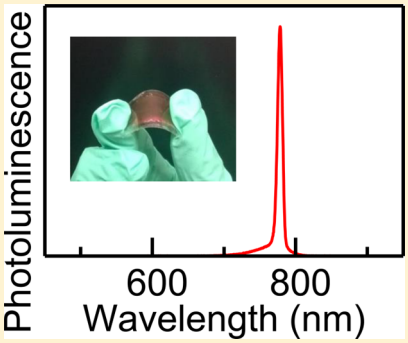

KEYWORDS: *Organic−inorganic perovskite, photoluminescence, lasing, passivation, cholesteric liquid crystal, flexible, amplified spontaneous emission*

Organic−inorganic perovskites are generating a great deal of excitement in the photovoltaic community with certified device power conversion of 20.1% recently demonstrated.[1−8] The crystal structure of the perovskite family of materials takes the form ABX_3, and the hybrid perovskites of recent interest are composed of an organic cation (A = $CH_3NH_3^+$ or $HC(NH_2)_2^+$),[9,10] a metal cation (B = Pb^{2+} or Sn^{2+}),[6,11,12] and halides (X = I^-, Br^-, or Cl^-)[6]. These components can be interchanged to allow tuning of the electronic band gap from ~1.3 eV to ~3.0 eV.[10,11,13] Their high performance is in part due to long carrier diffusion lengths,[14,15] large extinction coefficients, and a sharp optical band edge, suggesting low levels of disorder.[16,17] Their performance can also be attributed to the presence of efficient radiative bimolecular recombination of free electrons and holes.[18−20] These radiative processes become dominant at higher charge densities (>10^{16} cm^{-3}), with photoluminescence (PL) quantum efficiencies of up to 70% at room temperature and approaching 100% at low temperature having already been reported.[18,19]

Minimizing the fraction of recombination that is nonradiative is important for pushing the open-circuit voltages in photovoltaic devices toward thermodynamic limits.[21] Efficient radiative recombination also opens up the possibility of highly efficient light-emitting devices based on these perovskites. Perovskite light-emitting diodes (LEDs) were first demonstrated in the 1990s using two-dimensional perovskite structures that only showed electroluminescence (EL) at liquid nitrogen temperatures.[22−24] To achieve room-temperature EL, Mitzi and co-workers devised a scheme whereby a quaterthiophene diamine dye was used as both the organic cation and

Received: February 18, 2015
Revised: May 9, 2015
Published: May 19, 2015

DOI: 10.1021/acs.nanolett.5b00678
Nano Lett. 2015, 15, 4935−4941

emissive component, but the emission was not from the perovskite sheets themselves.[25] Tan et al. recently demonstrated the first LEDs utilizing these three-dimensional $CH_3NH_3PbX_3$ perovskites, reporting room temperature internal quantum efficiencies (IQEs) of ~3%.[37] Recently, Deschler et al. and separately Xing et al. reported a narrowing of the emission spectrum in thin films of $CH_3NH_3PbX_3$ perovskites at room temperature due to amplified spontaneous emission (ASE),[19,26] a phenomenon that occurs for the guided wave modes that propagate freely in-plane.[27] Deschler et al. also observed out-of-plane cavity modes at room temperature under pulsed laser excitation from a vertical cavity in which the perovskite was sandwiched between a gold mirror and a Bragg reflector, and multimode lasing was observed above a threshold of ~50 $\mu J/cm^2$/pulse. Optically pumped lasing has also been recently achieved at room temperature in polygonal nanocavities[28,29] and spherical resonators,[30] as well as random lasing from microcrystal networks,[31] beckoning the emergence of a new field in perovskite research.[1]

Chiral nematic (cholesteric) liquid crystals (CLCs) are a liquid crystalline phase that spontaneously self-organizes to form a macroscopic helicoidal structure.[32] When the pitch (the length scale that defines the periodicity of the structure) of the CLC helix is on the order of the wavelength of visible light, vivid Bragg reflection can be observed. With the advent of high twisting power chiral additives, it is now possible through simple means to form CLC phases with a Bragg reflection centered at any desired wavelength ranging from the ultraviolet to the infrared.[32] Furthermore, CLC polymers can be spin-coated onto a range of substrates including flexible structures. The use of CLCs instead of conventional inorganic Bragg reflectors[19] could potentially simplify the fabrication procedure and would provide a facile means with which to access a range of wavelengths simultaneously (e.g., through pitch gradients[33,34]) that is not necessarily readily achievable with other forms of Bragg reflector.

Here, we demonstrate enhanced optically pumped ASE from the $CH_3NH_3PbI_3$ perovskite when the material is sandwiched within a cavity composed of a CLC polymer reflector on glass, an alumina underlayer, and a metal back reflector. We find that the threshold for ASE from the perovskite in the device stack is lowered by at least two orders of magnitude compared to films without the CLC layer, and reduced even further for deposition on flexible substrates, resulting in a factor of two reduction in threshold fluence for gain narrowing compared to previous reports.[19,26,30] With further improvements to the quality factor and reflectivity of the CLC layer, the device structure is particularly promising for the development of a potentially wavelength-tunable single-mode "mirror-less" laser for use in a range of photonic applications.

To fabricate a controllable device stack, we use a compact layer of Al_2O_3 (c-Al_2O_3), deposited by controlled atomic layer deposition (ALD), as a transparent insulating spacer layer between the CLC (on glass) and the perovskite film. Films of $CH_3NH_3PbI_3$ of thickness ~50 nm were produced on substrates using the vapor-assisted solution processing (VASP) method reported in detail elsewhere.[35] Briefly, 50 nm of PbI_2 was thermally evaporated onto the substrate and then converted to the perovskite by exposing the film to methylammonium iodide (MAI) vapor. The films were spin-coated with the insulating polymer poly(methyl methacrylate) (PMMA) to protect them from air and moisture (see Supporting Information for full experimental methods).[14,36]

Figure 1 shows the time-resolved PL decays of the perovskite deposited on bare glass (blue) and on a dense compact 170 nm

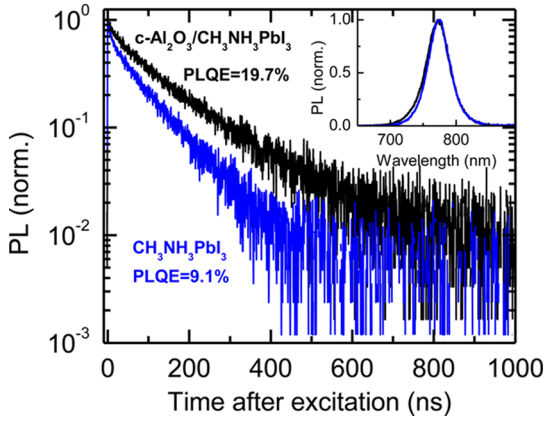

Figure 1. Time-resolved PL decays from the perovskite coated on neat glass ($CH_3NH_3PbI_3$; blue) and on compact Al_2O_3 (c-Al_2O_3/$CH_3NH_3PbI_3$; black), both with top layers of the insulating polymer PMMA. Samples were photoexcited with pulsed excitation (510 nm, 1 MHz repetition rate, 117 ps pulse length, 0.03 $\mu J/cm^2$/pulse), and the emission was detected at 780 nm. The measured PLQE values are labeled on the plot. Inset: steady-state PL spectra of the samples.

layer of Al_2O_3 (black), with pulsed photoexcitation of the samples at a wavelength of 510 nm and emission collected at 780 nm. We find that the PL lifetime of the perovskite is extended when it is deposited on the alumina underlayer. In addition, the photoluminescence quantum efficiency (PLQE) comparably increases from 9.1% for the neat film to 19.7% for the film deposited on alumina. These results are consistent with those reported by Tan et al., who found a substantial increase in LED quantum efficiency when inserting a thin alumina underlayer, which they attributed both to suppressed luminescence quenching at their device junction and also to the surface-induced structuring of the perovskite layer.[37] We speculate that the influence of the substrate upon both crystallization and generation of surface defects is playing a role here.[38,39] In addition, the previously observed "n-doping" from mesoporous alumina may also occur to a lesser extent at a planar interface,[40] which would result in filling of nonradiative electronic trap sites at this interface. These results suggest that c-Al_2O_3 is a highly suitable choice for the spacer layer.

We next built up the full device stack shown in Figure 2, panel a. The CLC layer (~7 μm) was fabricated by spin coating the CLC mixture on a rubbed polyimide glass plate. The reflection peak of CLC was centered at ~780 nm so that the center of the reflection band matched the peak emission wavelength of the perovskite ($\lambda \approx 780$ nm) while remaining transparent to the pump beam (530 nm) (Figure 2b). To maximize amplification of the perovskite emission within the 50 nm perovskite layer, we sandwich the perovskite between two transparent spacer layers: an underlying 170 nm layer of Al_2O_3 as described above, and a ~170 nm spin-coated top layer of the insulating polymer PMMA, to make a ~390 nm ($\sim\lambda/2$) thick Fabry–Perot resonator cavity. The stack was completed by thermally evaporating a gold back reflector (75 nm), which reflects both the perovskite emission and the optical pump, thus allowing for a second pass of the pump and thereby increasing the absorption in the perovskite. We show a scanning electron microscope (SEM) cross-section of the layers of the stack in

DOI: 10.1021/acs.nanolett.5b00678
Nano Lett. 2015, 15, 4935–4941

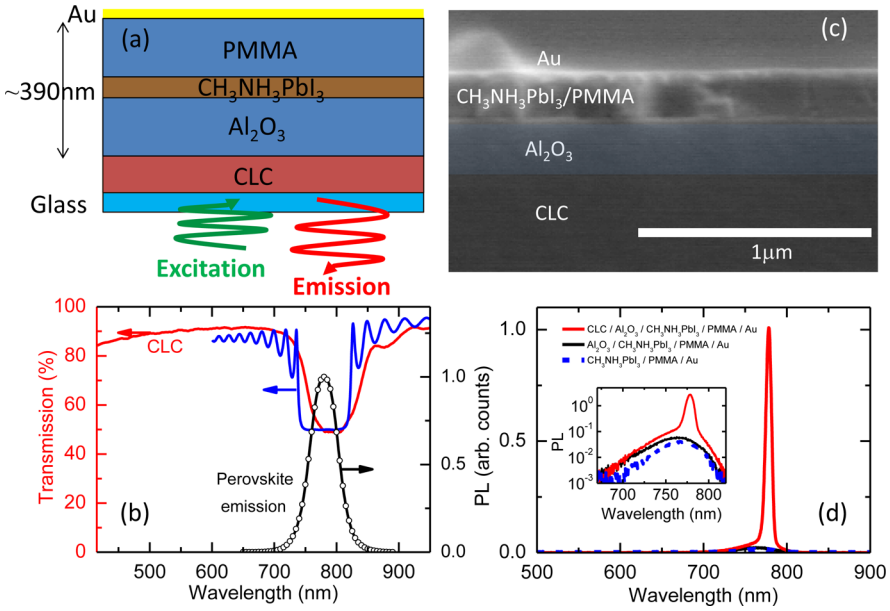

Figure 2. (a) Schematic of the device stack. (b) Transmission spectrum of the CLC reflector on glass (left axis) with PL spectrum from the perovskite thin film overlaid (black circles, right axis). The blue line shows the modeled transmission spectrum of the device stack using the 4 × 4 Berreman matrix approach. (c) SEM cross-section image of the full device structure on glass. The alumina layer has been shaded for contrast. (d) Emission from full device stack (red), stack without CLC (black), and stack without CLC and alumina (blue dashed), with pulsed excitation (530 nm, 4 ns pulses, 10-Hz repetition rate, ~60 μJ/cm^2/pulse).

Figure 2, panel c, and we show the transmission spectrum of the device stack modeled using the 4 × 4 Berreman matrix approach designed for anisotropic media in Figure 2, panel b (blue line).[41] We note here that depositing on the CLC with alumina by ALD or processing the perovskite by the VASP method (as presented here) or by solution-processing (not shown here) did not in any way degrade the CLC layer or alter its properties, suggesting the CLC layer is robust to a variety of processing conditions. We also note that, through a combination of polarizing optical microscopy and transmission measurements, we did not observe any birefringence in the perovskite, which would otherwise scramble the polarization of the light in the stack thereby potentially making the CLC reflector ineffective.

We show the emission from the stack with pulsed excitation (530 nm, 4 ns pulses, 10-Hz repetition rate, ~60 μJ/cm^2/pulse) in Figure 2, panel d. We see ASE from the sample with the full device stack (CLC/Al_2O_3/$CH_3NH_3PbI_3$/PMMA/Au; red spectrum), whereas we only observe PL from the identical sample without the CLC layer (Al_2O_3/$CH_3NH_3PbI_3$/PMMA/Au; black) and with the neat perovskite film deposited on glass ($CH_3NH_3PbI_3$/PMMA/Au; blue). We attribute the emission narrowing as a result of the CLC layer to be due to ASE rather than other narrowing mechanisms, such as superfluorescence or excitonic effects,[42,43] which we would not expect to be affected by the addition of the CLC layer. Additionally, we rule out excitonic effects because of the low exciton binding energies in these materials.[44,45] We note that the trend of increasing PL intensity with the underlying Al_2O_3 layer is consistent with that reported in Figure 1. We also note that the emission from the device stack and control films does not exhibit any degree of polarization (see Supporting Information).

Figure 3, panel a shows the pump-dependent emission from the full device stack (glass/CLC/Al_2O_3/$CH_3NH_3PbI_3$/PMMA/Au) through a range of excitation fluences at room temperature. At a threshold fluence of ~10 μJ/cm^2/pulse, the emission changes from a broad PL (FWHM of ~0.1 eV) at low fluence to ASE (FWHM of ~0.01 eV) at high fluence. In contrast, the corresponding control stack without the CLC layer (glass/Al_2O_3/$CH_3NH_3PbI_3$/PMMA/Au) only shows broad PL even at the highest excitation fluence (600 μJ/cm^2/pulse; dashed green line). We note here that we have also observed ASE from highly emissive control films, but the use of CLCs consistently yielded stronger ASE and at a much lower threshold. ASE occurs for the guided wave modes that propagate freely in-plane,[27] and therefore we would not necessarily expect a vertical cavity to lower the ASE threshold. We believe that, in this case, the role the CLC reflector layer plays is to redirect the emission that propagates along the out-of-plane and oblique paths back into the bulk. As a result, the optical path length in the medium is increased, resulting in a lower ASE threshold when compared with the non-CLC substrates. Here, the CLC layer is effectively improving the waveguiding capability of the perovskite film. It is also possible that the out-of-plane cavity modes are also contributing to the gain narrowing we have seen here.[43]

The results for the full device stack measured at a temperature of 200 K are shown in the Supporting Information. We observe a general narrowing of the PL linewidths, a slight red-shift (~20−30 meV), and an increase in absolute emission intensity compared to the 300 K data, consistent with previous reports.[18,26,45,46]

For both temperatures, increasing the excitation fluence results in a transition from a broad PL spectrum to a much narrower ASE feature at a fluence of ~10−20 μJ/cm^2/pulse. The emission intensity at T = 300 K is plotted in Figure 3, panel c and is used to extract a transition fluence of 15.3 μJ/cm^2/pulse. These values are consistent with the values of ~10−20 μJ/cm^2/pulse reported by Xing et al. and Deschler et al. for $CH_3NH_3PbI_3$ in related stacks or even highly emissive thin films.[19,26] We extract a lower ASE threshold fluence of 6.2 μJ/cm^2/pulse for T = 200 K (see Supporting Information), which

DOI: 10.1021/acs.nanolett.5b00678
Nano Lett. 2015, 15, 4935−4941

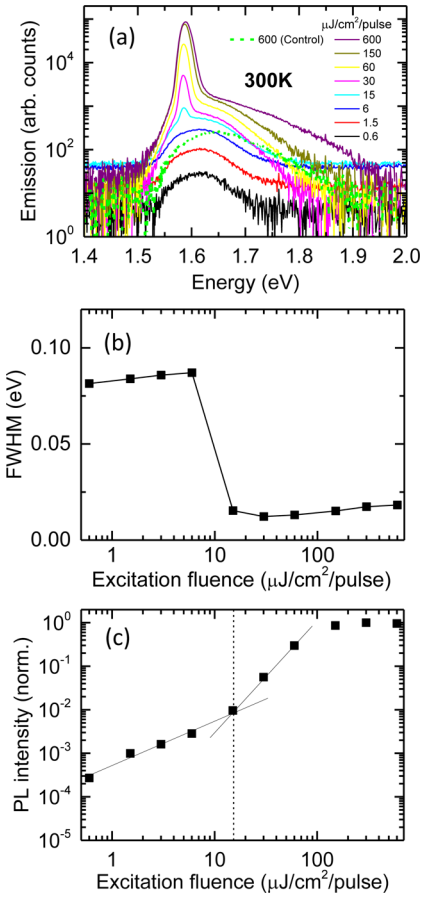

Figure 3. (a) Emission from the full device stack (glass/CLC/Al_2O_3/$CH_3NH_3PbI_3$/PMMA/Au) following photoexcitation (530 nm, 4 ns pulses, 10-Hz repetition rate) at a range of fluences. Emission from the control without the CLC (glass/Al_2O_3/$CH_3NH_3PbI_3$/PMMA/Au) is also shown for the highest excitation fluence (600 μJ/cm^2/pulse). Emission (b) FWHM and (c) intensity, with the extracted ASE threshold fluence (15.3 μJ/cm^2/pulse) denoted by the black dashed line. The spectral resolution of the detector setup at the measurement wavelength was ~6 meV (~1.8 nm). We did not observe visible sample degradation (photobleaching) until fluences of as high as ~10 mJ/cm^2/pulse.

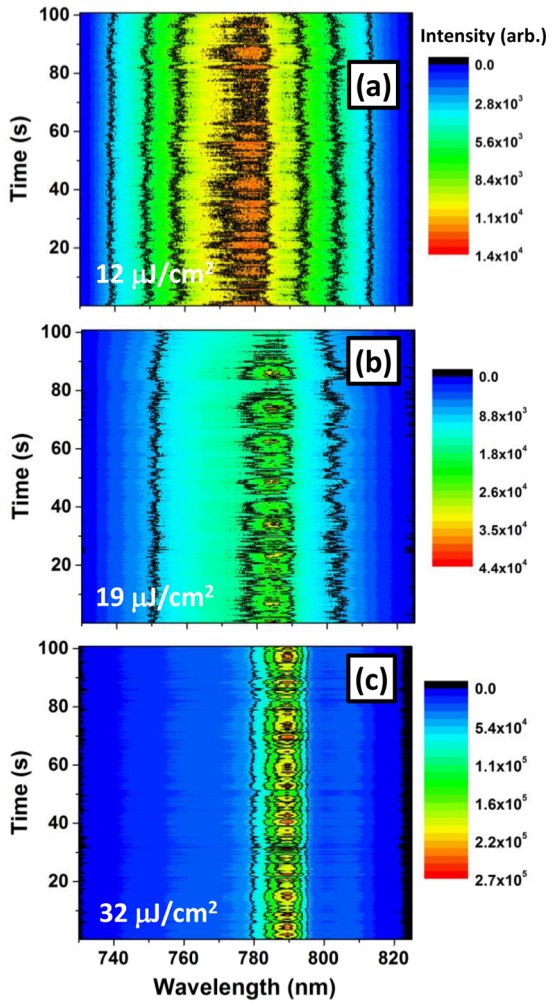

Figure 4. Temporal evolution of the emission spectra from the full device stack measured with a 6 Hz acquisition rate. The samples were photoexcited with 530 nm pulses of length 100 fs, 1-kHz repetition rate, 300-μm spot size, and a 30 ns detection window, with fluences (a) below (12 μJ/cm^2/pulse), (b) near (19 μJ/cm^2/pulse), and (c) above (32 μJ/cm^2/pulse) the ASE threshold.

is consistent with the observation of a higher PLQE at lower temperature that we have reported previously.[18] We observe that the FWHM and emission intensity both saturate at higher fluences at both temperatures, and a further increase in the fluence does not appear to result in a further collapse of the linewidth.

Following experimental evidence that the ASE threshold decreases with the addition of the CLC layer, we monitored the temporal variation of the ASE mode distribution in the full device stack. Figure 4 shows "snapshots" (gate-length 30 ns) of the emission profile with 6 Hz sampling rate following pulsed excitation at 530 nm (100 fs pulse length, 1-kHz repetition rate, 30 ns detection window after pulse) at various excitation fluences. Below the ASE threshold (Figure 4a; 12 μJ/cm^2/pulse), the emission is broad and featureless. At fluences close to the ASE threshold (Figure 4b; 19 μJ/cm^2/pulse), the shape of the emission changes, and a peak in the red tail of the emission spectrum evolves. At fluences above the ASE threshold (Figure 4c; 32 μJ/cm^2/pulse), this peak increases in intensity and slightly redshifts further. It is clear that there are fluctuations in the mode distribution over time; we observe temporal and spectral fluctuations in the ASE (Figure 4b,c) with modes being mostly observed only during one snapshot, without sustainable lasing.

The results presented above suggest that the emission from the device stacks above is unstable ASE and not lasing, and further refinement of the device stack will be required to achieve single mode lasing. The instability could be due to the relatively low quality factor of these CLC layers and because the CLC only reflects 50% of linearly polarized light. Therefore, the losses will be much higher here than in a conventional Bragg reflector. In addition, the nonuniformity of the device thickness caused by the current method to spin-coat PMMA may not allow the precise thickness control required for amplifying a single mode, although the desired thickness may be achieved in the current devices in some local areas where this thickness is achieved. Recent advances in methods to solution-process perovskites[47−50] and other materials such as PMMA[51] have yielded ultrasmooth layers, and therefore an entirely solution-processed device with minimal thickness variation could be feasibly fabricated. A more optimized stack accounting for the refractive indices (n) of the layers would consist of the ~50 nm

DOI: 10.1021/acs.nanolett.5b00678
Nano Lett. 2015, 15, 4935−4941

perovskite layer ($n \approx 2.3$ at ~780 nm[52]) sandwiched between ~80 nm of Al_2O_3 ($n \approx 1.75$) and ~80 nm of PMMA ($n \approx 1.5$), giving an optical path length of $\lambda/2$~390 nm. The saturation of the FWHM and emission intensity at high fluences (Figure 3b,c) suggests the absorption becomes saturated, and no further increase in excitation density can be achieved. Therefore, we expect that lasing could be achieved if the quality of the cavity was improved.

To test how the ASE threshold could further reduce with higher reflectivity substrates, we fabricated an 80% reflector by spin coating the CLCs on both sides of a half-wave film (see Supporting Information).[53,54] Here, the fraction of the unpolarized perovskite emission with the same handedness as the CLC on top of the half-wave film will be reflected, whereas light of the opposite handedness will be transmitted through the CLC. The transmitted light from the top CLC layer will change its handedness while it passes through the half-wave film (π phase shift) and will be further reflected by the CLC on the bottom side of the film, yielding a net reflectivity of up to ~80%.[43] The compound substrate is free-standing and flexible, which allows us to additionally demonstrate the versatility of these reflectors. Because of the temperature sensitivity of the wave plate, we omitted the ALD layer and instead first deposited a ~50 nm layer of PMMA by spin-coating, followed by a 300 nm layer of mixed halide perovskite ($CH_3NH_3PbI_{3-x}Cl_x$) by coevaporation,[55] which allows for a lower annealing temperature of 100 °C for a shorter period of time, and finally another ~50 nm spin-coated layer of PMMA. A photograph of the flexible device stack is shown in the inset of Figure 5. We plot the emission intensity as a function of

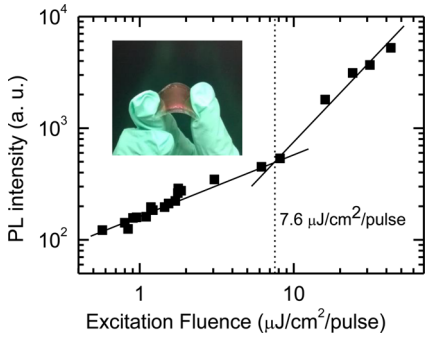

Figure 5. Extracted emission intensity from a device stack fabricated on a flexible 80% CLC reflector following photoexcitation at a range of fluences (532 nm, 5 ns pulses, 100-Hz repetition rate). The ASE transition fluence is determined to be 7.6 μJ/cm^2/pulse. Inset: photograph of the flexible device.

excitation fluence in Figure 5, where the ASE threshold has indeed been reduced further to 7.6 μJ/cm^2/pulse (cf. 15.3 μJ/cm^2/pulse for the 50% reflector). We note that the reduction in threshold is primarily attributed to the improved reflector because we again do not observe ASE up to the maximum pump intensity from the control sample (without the CLC), which was also prepared using coevaporation (see Supporting Information for PL spectra and FWHM data) or when using thicker (~300 nm) perovskite films with the 50% reflectors. This reduction in ASE threshold is highly encouraging, and it is expected that further improvements in the reflector quality and reflectivity (e.g., beyond 99%) will allow us to achieve sufficient amplification of the out-of-plane perovskite emission for lasing in these structures. We expect that the limitations in reflectivity of the CLC layers are predominantly practical, and further work into the deposition of these novel CLC layers will lead to further reflectivity improvements. For example, use of multiple stacks of left- and right-handed CLCs could result in much higher reflectivities.[43]

Furthermore, the perovskite emission wavelength is easily tunable by substituting different cations or anions; for example, by increasing the bromide content, the emission maximum blue-shifts toward the green, and additional chloride doping can shift the emission further toward the blue region of the visible spectrum.[17,19,26] Likewise, the CLC reflector can be easily designed to match the perovskite emission peak across this range of possible emission colors by changing the concentration of chiral additive.[56] The CLC could also be processed on top of the dielectric stack, which would remove the need for the Au back reflector and allow lasing from both ends of the cavity. However, we note that this will require alternative CLC fabrication methods to avoid methods for curing and mechanically rubbing the alignment layer that may damage the perovskite. The next logical steps are to pursue the avenues described above to optimize the devices to demonstrate a single-mode solution-processed perovskite laser.

In conclusion, we have investigated CLC reflectors as a means to enhance the line narrowing and ASE from organic–inorganic perovskite thin films toward lasing in these structures. We fabricated layered devices and observed perovskite ASE enhancement in stacks containing the CLC layer and have confirmed that these effects were not reliably seen in control devices without the CLC. We found ASE thresholds of ~7 μJ/cm^2/pulse on flexible CLC reflectors, which are lower than values reported elsewhere.[19,26] The work suggests a promising route to single-mode "mirror-less" lasing from perovskite materials with the CLC providing additional potential functionality, such as flexible substrates and allowing wavelength-tunability, in addition to acting as the reflector. Flexible lasers may find use in flexible displays or military applications such as friend or foe identification.

■ ASSOCIATED CONTENT

Supporting Information

Full experimental methods, low temperature device stack measurements, additional characterization and description of the 80% reflector devices, and polarization checks. The Supporting Information is available free of charge on the ACS Publications website at DOI: 10.1021/acs.nanolett.5b00678.

■ AUTHOR INFORMATION

Corresponding Authors

*E-mail: stranks@mit.edu.
*E-mail: stephen.morris@eng.ox.ac.uk.
*E-mail: h.snaith1@physics.ox.ac.uk.

Present Address

(S.D.S.) Research Laboratory of Electronics, Massachusetts Institute of Technology, 77 Massachusetts Avenue, Cambridge, Massachusetts 02139, United States.

Author Contributions

The project was conceived, planned, and coordinated by S.D.S. (supervised by H.J.S.), S.M.M., S.M.W. (supervised by S.M.M. and S.J.E.), M.K.R., and H.J.S. The CLC reflectors were prepared by H.K. (supervised by A.P.H.J.S. and M.G.D.). S.D.S. and S.M.W. fabricated the device stacks and performed the

DOI: 10.1021/acs.nanolett.5b00678
Nano Lett. 2015, 15, 4935–4941

optical characterization, with additional temporal characterization performed by F.D. K.W. (supervised by H.J.S.) took scanning electron microscopy images and assisted with additional fabrication. J.B.P. (supervised by M.B.J. and L.M.H.) grew the perovskite layers via dual source vapor deposition, and M.S. (supervised by H.J.S.) and S.M.W. characterized the resulting stacks. S.D.S. and S.M.W. wrote the manuscript with contributions from all authors.

Notes

The authors declare no competing financial interest.

■ ACKNOWLEDGMENTS

The research leading to these results has received funding from the European Union Seventh Framework Programme [FP7/2007-2013] under Grant Agreement No. 604032 of the MESO project. The authors thank Dr. Henning Urban for assistance with ALD, Dr. Martina Congiu for assistance with perovskite preparation, and Jin Zhang for preparing the precursor salts. S.M.M. gratefully acknowledges The Royal Society for financial support, and F.D. acknowledges funding from the Herschel Smith Research Fellowship. The research in Eindhoven was financially supported by the Dutch Polymer Institute (DPI), Project No. 764. J.B.P. thanks the Engineering and Physical Sciences Research Council and Merck Chemicals for financial support through an Industrial CASE studentship. The authors thank Professor Sir Richard Friend for helpful discussions.

■ REFERENCES

(1) Stranks, S. D.; Snaith, H. J. *Nat. Nanotechnol.* **2015**, *10*, 391−402.
(2) Green, M. A.; Ho-Baillie, A.; Snaith, H. J. *Nat. Photonics* **2014**, *8*, 506−514.
(3) Gratzel, M. *Nat. Mater.* **2014**, *13*, 838−842.
(4) Lee, M. M.; Teuscher, J.; Miyasaka, T.; Murakami, T. N.; Snaith, H. J. *Science* **2012**, *338*, 643−647.
(5) Kim, H. S.; Lee, C. R.; Im, J. H.; Lee, K. B.; Moehl, T.; Marchioro, A.; Moon, S. J.; Humphry-Baker, R.; Yum, J. H.; Moser, J. E.; Gratzel, M.; Park, N. G. *Sci. Rep.* **2012**, *2*, 591.
(6) Kojima, A.; Teshima, K.; Shirai, Y.; Miyasaka, T. *J. Am. Chem. Soc.* **2009**, *131*, 6050−6051.
(7) Ito, S.; Tanaka, S.; Vahlman, H.; Nishino, H.; Manabe, K.; Lund, P. *ChemPhysChem* **2014**, *15*, 1194−1200.
(8) Zhou, H.; Chen, Q.; Li, G.; Luo, S.; Song, T.-b.; Duan, H.-S.; Hong, Z.; You, J.; Liu, Y.; Yang, Y. *Science* **2014**, *345*, 542−546.
(9) Lee, J. W.; Seol, D. J.; Cho, A. N.; Park, N. G. *Adv. Mater.* **2014**, *26*, 4991−4998.
(10) Eperon, G. E.; Stranks, S. D.; Menelaou, C.; Johnston, M. B.; Herz, L. M.; Snaith, H. J. *Energy Environ. Sci.* **2014**, *7*, 982−988.
(11) Noel, N. K.; Stranks, S. D.; Abate, A.; Wehrenfennig, C.; Guarnera, S.; Haghighirad, A. A.; Sadhanala, A.; Eperon, G. E.; Pathak, S. K.; Johnston, M. B.; Petrozza, A.; Herz, L. M.; Snaith, H. J. *Energy Environ. Sci.* **2014**, *7*, 3061−3068.
(12) Hao, F.; Stoumpos, C. C.; Cao, D. H.; Chang, R. P. H.; Kanatzidis, M. G. *Nat. Photonics* **2014**, *8*, 489−494.
(13) Kitazawa, N.; Watanabe, Y.; Nakamura, Y. *J. Mater. Sci.* **2002**, *37*, 3585−3587.
(14) Stranks, S. D.; Eperon, G. E.; Grancini, G.; Menelaou, C.; Alcocer, M. J.; Leijtens, T.; Herz, L. M.; Petrozza, A.; Snaith, H. J. *Science* **2013**, *342*, 341−344.
(15) Xing, G.; Mathews, N.; Sun, S.; Lim, S. S.; Lam, Y. M.; Gratzel, M.; Mhaisalkar, S.; Sum, T. C. *Science* **2013**, *342*, 344−347.
(16) De Wolf, S.; Holovsky, J.; Moon, S.-J.; Löper, P.; Niesen, B.; Ledinsky, M.; Haug, F.-J.; Yum, J.-H.; Ballif, C. *J. Phys. Chem. Lett.* **2014**, *5*, 1035−1039.
(17) Sadhanala, A.; Deschler, F.; Thomas, T. H.; Dutton, S. E.; Goedel, K. C.; Hanusch, F. C.; Lai, M. L.; Steiner, U.; Bein, T.; Docampo, P.; Cahen, D.; Friend, R. H. *J. Phys. Chem. Lett.* **2014**, *5*, 2501−2505.
(18) Stranks, S. D.; Burlakov, V. M.; Leijtens, T.; Ball, J. M.; Goriely, A.; Snaith, H. J. *Phys. Rev. Appl.* **2014**, *2*, 034007.
(19) Deschler, F.; Price, M.; Pathak, S.; Klintberg, L. E.; Jarausch, D.-D.; Higler, R.; Hüttner, S.; Leijtens, T.; Stranks, S. D.; Snaith, H. J.; Atatüre, M.; Phillips, R. T.; Friend, R. H. *J. Phys. Chem. Lett.* **2014**, *5*, 1421−1426.
(20) Manser, J. S.; Kamat, P. V. *Nat. Photonics* **2014**, *8*, 737−743.
(21) Miller, O. D.; Yablonovitch, E.; Kurtz, S. R. *IEEE J. Photovoltaics* **2012**, *2*, 303−311.
(22) Era, M.; Morimoto, S.; Tsutsui, T.; Saito, S. *Appl. Phys. Lett.* **1994**, *65*, 676−678.
(23) Hattori, T.; Taira, T.; Era, M.; Tsutsui, T.; Saito, S. *Chem. Phys. Lett.* **1996**, *254*, 103−108.
(24) Hong, X.; Ishihara, T.; Nurmikko, A. V. *Solid State Commun.* **1992**, *84*, 657−661.
(25) Chondroudis, K.; Mitzi, D. B. *Chem. Mater.* **1999**, *11*, 3028−3030.
(26) Xing, G.; Mathews, N.; Lim, S. S.; Yantara, N.; Liu, X.; Sabba, D.; Gratzel, M.; Mhaisalkar, S.; Sum, T. C. *Nat. Mater.* **2014**, *13*, 476−480.
(27) Friend, R. H.; Denton, G. J.; Tessler, N.; Stevens, M. A. *Adv. Mater.* **1997**, *9*, 547−551.
(28) Zhang, Q.; Ha, S. T.; Liu, X.; Sum, T. C.; Xiong, Q. *Nano Lett.* **2014**, *14*, 5995−6001.
(29) Liu, X.; Ha, S. T.; Zhang, Q.; de la Mata, M.; Magen, C.; Arbiol, J.; Sum, T. C.; Xiong, Q. *ACS Nano* **2015**, *9*, 687−695.
(30) Sutherland, B. R.; Hoogland, S.; Adachi, M. M.; Wong, C. T.; Sargent, E. H. *ACS Nano* **2014**, *8*, 10947−10952.
(31) Dhanker, R.; Brigeman, A. N.; Larsen, A. V.; Stewart, R. J.; Asbury, J. B.; Giebink, N. C. *Appl. Phys. Lett.* **2014**, *105*, 151112.
(32) Coles, H.; Morris, S. *Nat. Photonics* **2010**, *4*, 676−685.
(33) Broer, D. J.; Lub, J.; Mol, G. N. *Nature* **1995**, *378*, 467−469.
(34) Broer, D. J.; Mol, G. N.; Haaren, J. A. M. M. V.; Lub, J. *Adv. Mater.* **1999**, *11*, 573−578.
(35) Chen, Q.; Zhou, H.; Hong, Z.; Luo, S.; Duan, H. S.; Wang, H. H.; Liu, Y.; Li, G.; Yang, Y. *J. Am. Chem. Soc.* **2014**, *136*, 622−625.
(36) Habisreutinger, S. N.; Leijtens, T.; Eperon, G. E.; Stranks, S. D.; Nicholas, R. J.; Snaith, H. J. *Nano Lett.* **2014**, *14*, 5561−5568.
(37) Tan, Z. K.; Moghaddam, R. S.; Lai, M. L.; Docampo, P.; Higler, R.; Deschler, F.; Price, M.; Sadhanala, A.; Pazos, L. M.; Credgington, D.; Hanusch, F.; Bein, T.; Snaith, H. J.; Friend, R. H. *Nat. Nanotechnol.* **2014**, *9*, 687−692.
(38) Noel, N. K.; Abate, A.; Stranks, S. D.; Parrott, E. S.; Burlakov, V. M.; Goriely, A.; Snaith, H. J. *ACS Nano* **2014**, *8*, 6815−6821.
(39) Wojciechowski, K.; Stranks, S. D.; Abate, A.; Sadoughi, G.; Sadhanala, A.; Kopidakis, N.; Rumbles, G.; Li, C. Z.; Friend, R. H.; Jen, A. K.; Snaith, H. J. *ACS Nano* **2014**, *8*, 12701−12709.
(40) Leijtens, T.; Stranks, S. D.; Eperon, G. E.; Lindblad, R.; Johansson, E. M.; McPherson, I. J.; Rensmo, H.; Ball, J. M.; Lee, M. M.; Snaith, H. J. *ACS Nano* **2014**, *8*, 7147−7155.
(41) Berreman, D. W. *J. Opt. Soc. Am.* **1972**, *62*, 502−510.
(42) McGehee, M. D.; Heeger, A. J. *Adv. Mater.* **2000**, *12*, 1655−1668.
(43) Jeong, S. M.; Sonoyama, K.; Takanishi, Y.; Ishikawa, K.; Takezoe, H.; Nishimura, S.; Suzaki, G.; Song, M. H. *Appl. Phys. Lett.* **2006**, *89*, 241116.
(44) Lin, Q.; Armin, A.; Nagiri, R. C. R.; Burn, P. L.; Meredith, P. *Nat. Photonics* **2014**, *9*, 106−112.
(45) D'Innocenzo, V.; Grancini, G.; Alcocer, M. J.; Kandada, A. R.; Stranks, S. D.; Lee, M. M.; Lanzani, G.; Snaith, H. J.; Petrozza, A. *Nat. Commun.* **2014**, *5*, No. 3586.
(46) Wehrenfennig, C.; Liu, M. Z.; Snaith, H. J.; Johnston, M. B.; Herz, L. M. *Apl Mater.* **2014**, *2*, 081513.
(47) Stranks, S. D.; Nayak, P. K.; Zhang, W.; Stergiopoulos, T.; Snaith, H. J. *Angew. Chem. Int. Ed* **2015**, *54*, 3240−3248.
(48) Zhang, W.; Saliba, M.; Moore, D. T.; Pathak, S. K.; Horantner, M. T.; Stergiopoulos, T.; Stranks, S. D.; Eperon, G. E.; Alexander-

DOI: 10.1021/acs.nanolett.5b00678
Nano Lett. 2015, 15, 4935−4941

Webber, J. A.; Abate, A.; Sadhanala, A.; Yao, S.; Chen, Y.; Friend, R. H.; Estroff, L. A.; Wiesner, U.; Snaith, H. J. *Nat. Commun.* **2015**, *6*, No. 6142.
(49) Jeon, N. J.; Noh, J. H.; Kim, Y. C.; Yang, W. S.; Ryu, S.; Seok, S. I. *Nat. Mater.* **2014**, *13*, 897−903.
(50) Xiao, M.; Huang, F.; Huang, W.; Dkhissi, Y.; Zhu, Y.; Etheridge, J.; Gray-Weale, A.; Bach, U.; Cheng, Y. B.; Spiccia, L. *Angew. Chem., Int. Ed.* **2014**, *53*, 9898−9903.
(51) Walsh, C. B.; Franses, E. I. *Thin Solid Films* **2003**, *429*, 71−76.
(52) Ball, J. M.; Stranks, S. D.; Hoerantner, M.; Hüttner, S.; Zhang, W.; Crossland, E.; Ramirez, I.; Riede, M.; Johnston, M. B.; Friend, R.; Snaith, H. *Energy Environ. Sci.* **2015**, *8*, 602−609.
(53) Makow, D. M. *Appl. Opt.* **1980**, *19*, 1274−1277.
(54) Khandelwal, H.; Loonen, R. C. G. M.; Hensen, J. L. M.; Schenning, A. P. H. J.; Debije, M. G. *J. Mater. Chem. A* **2014**, *2*, 14622−14627.
(55) Liu, M.; Johnston, M. B.; Snaith, H. J. *Nature* **2013**, *501*, 395−398.
(56) Mulder, D. J.; Schenning, A. P. H. J.; Bastiaansen, C. W. M. *J. Mater. Chem. C* **2014**, *2*, 6695−6705.

DOI: 10.1021/acs.nanolett.5b00678
Nano Lett. 2015, 15, 4935−4941